Does Superoxide Channel between the Copper Centers in Peptidylglycine Monooxygenase? A New Mechanism Based on Carbon Monoxide Reactivity†

Shulamit Jaron and Ninian J. Blackburn*

Department of Biochemistry and Molecular Biology, Oregon Graduate Institute of Science and Technology, 20000 N. W. Walker Road, Beaverton, Oregon 97006-8921

Received June 11, 1999; Revised Manuscript Received August 23, 1999

ABSTRACT: Peptidylglycine monooxygenase (PHM) carries out the hydroxylation of the α-C atom of glycine-extended propeptides, the first step in the amidation of peptide hormones by the bifunctional enzyme peptidyl-α-amidating monooxygenase (PAM). Since PHM is a copper-containing monooxygenase, a study of the interaction between the reduced enzyme and carbon monoxide has been carried out as a probe of the interaction of the Cu(I) sites with O_2. The results show that, in the absence of peptide substrate, reduced PHM binds CO with a stoichiometry of 0.5 CO/Cu(I), indicating that only one of the two copper centers, Cu_B, forms a Cu(I)-carbonyl. FTIR spectroscopy shows a single band in the 2200−1950 cm^{-1} energy region with ν(CO) = 2093 cm^{-1} assigned to the intraligand C−O stretch via isotopic labeling with ^{13}CO. A His242Ala mutant of PHM, which deletes the Cu_B site by replacing one of its histidine ligands, completely eliminates CO binding. EXAFS spectroscopy is consistent with binding of a single CO ligand with a Cu−C distance of 1.82 ± 0.03 Å. The Cu−S(met) distance increases from 2.23 ± 0.02 Å in the reduced unliganded enzyme to 2.33 ± 0.01 Å in the carbonylated enzyme, suggesting that the methionine-containing Cu_B center is the site of CO binding. The binding of the peptide substrate N-Actyr-val-gly perturbs the CO ligand environment, eliciting an IR band at 2062 cm^{-1} in addition to the 2093 cm^{-1} band. ^{13}CO isotopic substitution assigns both frequencies as C−O stretching bands. The CO:Cu binding stoichiometry and peptide/CO FTIR titrations indicate that the 2062 cm^{-1} band is due to binding of CO at a second site, most likely at the Cu_A center. This suggests that peptide binding may activate the Cu_A center toward O_2 binding and reduction to superoxide. As a result of these findings, a new mechanism is proposed involving channeling of superoxide across the 11 Å distance between the two copper centers.

Many neuropeptides and peptide hormones are activated by posttranslational C-terminal amidation in a reaction that is carried out by the enzyme peptidyl-α-amidating monooxygenase (PAM,[1] EC 1.14.17.3) (*1*−*3*). PAM is a bifunctional enzyme which consists of two domains—the peptidyl-α-hydroxylating monooxygenase (PHM) and the peptidyl-α-hydroxyglycine lyase (PAL)—with separate enzymatic activities (*4*−*7*). The PHM domain catalyzes the first step of the reaction, in which the terminal glycine residue of a peptide is hydroxylated at the C_α position, in a copper, ascorbate, and molecular oxygen-dependent monooxygenation. The hydroxylated peptide is then cleaved through N−C bond fission by the PAL domain to form the amidated peptide in what is believed to be a Zn-dependent process (*8*). The two enzyme activities are encoded by a single-copy gene and can either be expressed as a single unit or as independent proteins (*9*). PHM shares similar cofactor requirements and a 30% homology in its amino acid sequence with another monooxygenase, dopamine-*β*-monooxygenase (D*β*M) (*10*). Although their substrate specificity is quite different, both PHM and D*β*M appear to share a number of mechanistic features (*11*, *12*), and they each contain two mononuclear coppers at their active sites which undergo redox cycling through Cu(II) and Cu(I) forms (*13*−*15*).

Spectroscopic studies (and in particular XAS) provided the first structural model of the active site of both the oxidized and reduced forms of PAM (*15*, *16*). EXAFS data were used to show that all five conserved histidines between the amino acid sequence of PHM and D*β*M (H107, H108, H172, H242, and H244) and one conserved methionine (M314) were ligands to the copper centers (*15*, *16*). Mutations to any one of these ligands produced an inactive enzyme (*16*−*18*). Further analysis of the EXAFS data suggested a copper coordination in the oxidized enzyme composed of two inequivalent mononuclear Cu(II) sites, designated Cu_A and Cu_B, with a $Cu_A(His)_3O\cdots Cu_B(His)_2O_2$ ligand distribution. Reduction led to dissociation of the bound solvent and the additional coordination of S from the methionine ligand at the Cu_B center (*15*). Proteolytic cleavage using endo lys-C was subsequently used to split the enzyme into two subdomains, each containing one copper center with proposed ligand sets (H107, H108, and H172) and

† This research was supported by Grant NS-27583 from the National Institutes of Health (to N.J.B.).

* To whom correspondence should be addressed. Phone: (503) 748-1384. Fax: (503) 748-1464. E-mail: ninian@bmb.ogi.edu.

[1] Abbreviations: CCO, cytochrome *c* oxidase; CSFM, complete serum-free medium; D*β*M, dopamine-*β*-monooxygenase; DW, Debye−Waller; EXAFS, extended X-ray absorption fine structure; FTIR, Fourier transform infrared; PAL, peptidyl-α-hydroxyglycine lyase; PAM, peptidyl-α-amidating monooxygenase; PHM, peptidylglycine monooxygenase; PHMcc, PHM catalytic core; wt, wild-type; XAS, X-ray absorption spectroscopy.

10.1021/bi991341w CCC: $18.00
Published on Web 10/23/1999

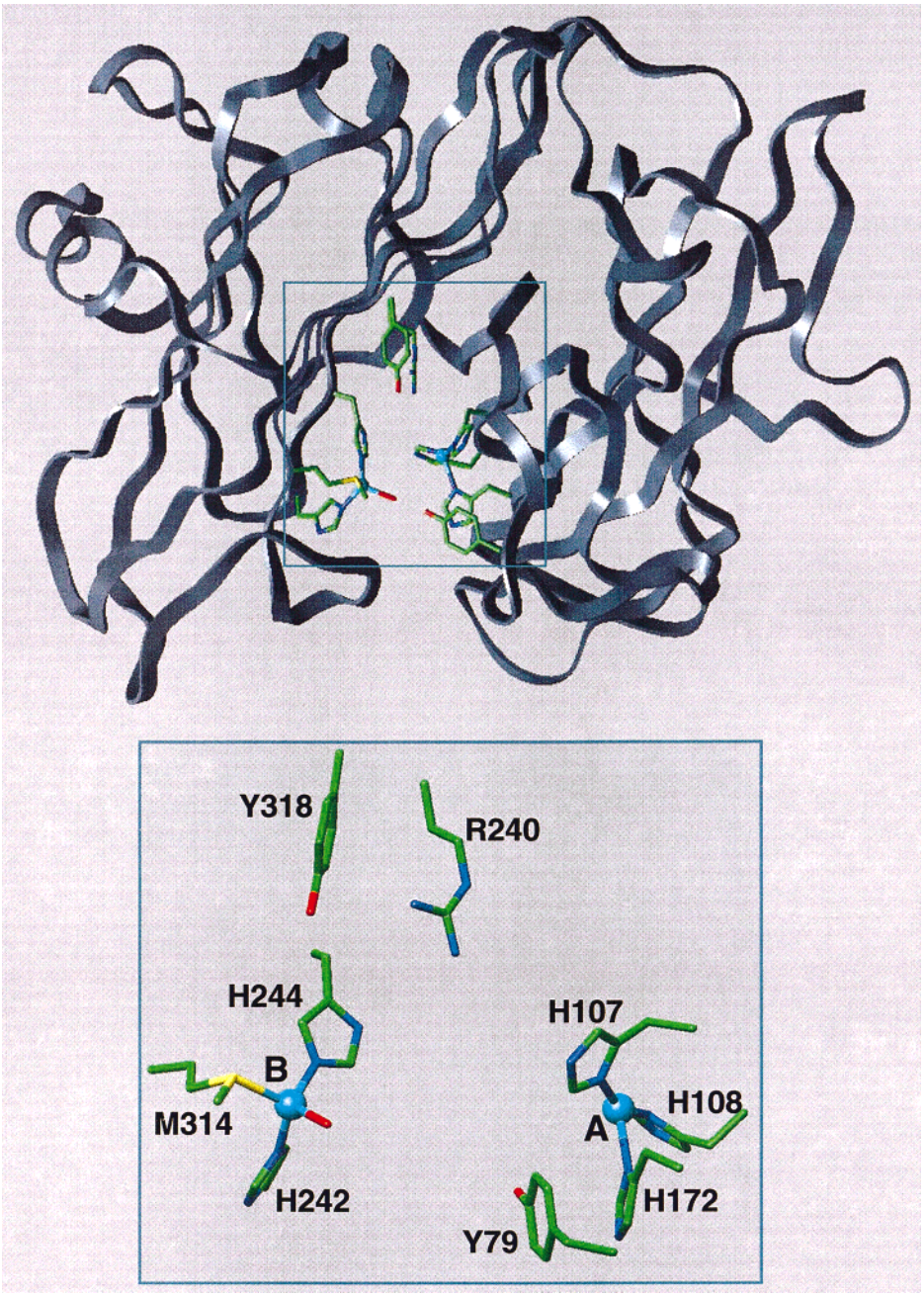

FIGURE 1: Ribbon diagram for the PHMcc crystal structure showing the position of the catalytic copper centers and important active site residues. The inset shows an exploded view of the active site. Taken from the 1PHM data set of PDB coordinates at 1.9 Å resolution (*19*).

(H242, H244, and M314), respectively (*18*).

These findings have been fully confirmed by the recent X-ray crystal structure of a truncated version of PHM, extending from residues 16 to 356 and designated PHM catalytic core (PHMcc) (*19*). The overall structure consists of two 150 residue domains, each a nine-stranded β-sandwich. Each domain binds a single catalytic copper, orienting it into the interdomain space which is completely accessible to solvent. Cu_A is bound to three histidines (H107, H108, and H172) from domain I in approximately T-shaped geometry, while Cu_B is located 11 Å distant, ligated by a solvent molecule, two histidines, and a methionine from domain II (H242, H244, and M314), in pseudo-tetrahedral geometry (Figure 1).

The crystal structure of PHM has allowed an intimate look at its active site, which has generated a proposal for the mechanism of catalytic events (*11*, *19*). In this mechanism, Cu^{2+} is first reduced to Cu^{1+} in two one-electron transfers to form the catalytically active dicopper(I) form. The subsequent binding of peptidyl-gly and molecular oxygen is equilibrium-ordered, which implies that the peptide substrate must bind prior to oxygen binding to ensure catalytic competence (*11*). The crystal structure shows the peptidyl-gly to be held in place by electrostatic interactions between the negatively charged C-terminal peptide carboxylate oxygens and the positively charged guanidinium group of R240 with an additional H-bond to the hydroxyl of the conserved Y318. This peptide-binding site is in domain II and is close to the oxygen-binding site at Cu_B [as previously suggested from XAS and CO binding data on a Cu_A depleted form of DβM (*20*)] with the pro-S C_α−H pointing directly at the solvent site on Cu_B. Thus, the crystal structure lends

strong support to a mechanism involving the formation of a hydroperoxide intermediate at Cu_B, followed by rapid hydroxylation of the peptide substrate which is perfectly aligned within the active site pocket. However, the structure gives no clue to how such an intermediate can be formed, since the copper centers are 11 Å apart and no through-bond electron-transfer pathway exists between them. The poor efficiency of electron transfer through disordered water (*21*) brings into question the previously accepted premise (*15*, *19*, *20*) that O_2 binding occurs at Cu_B and that its subsequent two-electron reduction (to form the hydroperoxide) involves long-range electron transfer between Cu_A and Cu_B (*12*). Some other mechanism for O_2 binding and reduction seems more likely.

Here we explore new mechanisms for O_2 binding and reduction in PHMcc via studies of CO binding to the reduced enzyme. CO has been used extensively as a model for oxygen binding to iron and copper proteins, since both ligands have empty π antibonding orbitals that are available for interactions with filled metal d-orbitals. CO and O_2 are also both neutral diatomic molecules with similar stereochemical binding requirements. Our results show that, in the absence of substrate, CO does indeed bind to Cu_B as has previously been observed for bifunctional PAM and DβM (*15*, *22*, *23*). However, we find that substrate binding to the enzyme turns on previously undetected CO reactivity at Cu_A. This result suggests a completely new and unprecedented mechanism for electron/proton transfer between the two metal centers involving initial reaction of dioxygen at Cu^I_A to form superoxide, followed by superoxide channeling between the two copper centers and subsequent reaction of $HO_2^\bullet$ at Cu^I_B to form the reactive hydroperoxy intermediate.

EXPERIMENTAL PROCEDURES

Preparation of Medium for Cell Culture. Minimal medium was prepared as follows. To 1 L of deionized (Nano-pure) water was added 1 packet α-MEM (Minimal Essential Medium), 1.23 g of Hepes, 1.35 g of glucose, 0.12 g of penicillin G, 0.2 g of streptomycin sulfate, and 0.6 g of glutamine. The pH was adjusted to 7.35, and the solution stirred for 30 min, after which 2.2 g of sodium bicarbonate was added. For serum-containing medium, 100 mL of dialyzed calf serum (Hyclone) was added to 900 mL of medium, and the solution was sterile filtered into 1 L glass or polycarbonate bottles. The medium was stored sterile at 4 °C.

DMEM/F12 [Dubelco's Modified Eagle Medium, Nutrient Mixture F-12 (Ham)] medium was prepared as above, except that a 1 L packet of DMEM/F12 was used instead of α-MEM. Serum-containing medium was prepared by adding 100 mL of fetal clone II (Hyclone) to 900 mL of medium, followed by sterile filtration into glass bottles. The medium was stored sterile at 4 °C.

Complete serum-free medium (CSFM) was prepared as above, except that the dialyzed calf serum or fetal clone II was omitted and 2.5 mg of insulin and 0.5 mg of transferrin were added per liter of medium. The solution was sterile filtered and stored at 4 °C.

Cell Lines and Cell Growth. The cell lines used to express and purify PHMcc were constructed and kindly provided to us by Drs. Richard E. Mains and Betty A. Eipper (Department of Neuroscience, The Johns Hopkins School of Medicine). The pCIS.PHMcc vector carrying the PHMcc gene was constructed and stably transfected into a Chinese hamster ovary (CHO) cell line DG44 (dhfr-) (created by Dr. L. A. Chasin, Columbia University). Full details are described by Eipper and co-workers (*18*). Frozen cells were thawed and grown initially on minimal medium (α-MEM, GIBCO), containing 10% dialyzed calf serum in order to ensure positive selection for cells that retained high copy numbers of the pCIS.PHMcc vector. After the first passage, the medium was changed to DMEM/F12 (GIBCO) containing 10% fetal clone II (Hyclone), which produced more rapid cell growth and higher rates of division than the minimal medium. Cell mass was amplified in NUNC triple flasks until a confluent area of 0.3−0.4 m^2 was achieved. At this point, the cells were trypsinized, resuspended in 75 mL of the DMEM/F12/fetal clone II serum-containing medium, and inoculated into a Cellmax 100 1.1 m^2 hollow-fiber bioreactor (Spectrum). In this system, the cell mass grows on the outside of hollow fiber capillaries through which oxygen-rich medium flows. Since the hollow fibers have a 4 kDa molecular mass cutoff, the secreted proteins, including PHMcc, concentrate in the extra capillary space and can be harvested daily.

The cell mass was grown for approximately 10 days on the serum-containing DMEM/F12/fetal clone II medium. The volume of medium circulated through the bioreactor was 1 L, and the medium was changed when the glucose level dropped below 50% and/or the pH dropped below 6.6. At 3 day intervals, the medium within the extra capillary space (in contact with the growing cell mass) was drained, and fresh DMEM/F12/fetal clone II-containing medium was introduced. After 10 days, the serum was eliminated from the medium, and the cells were switched to growth on CSFM. The extra capillary medium (∼60 mL) was harvested daily, but the initial 4−5 days of harvested medium was discarded, because activity levels typically rose sharply after about 1 week of operation. The bioreactor consumed 1 L of CSFM/day, and the average daily PHMcc production was approximately 7−10 mg.

Enzyme Isolation. In a typical enzyme isolation, 7 days of bioreactor harvest were combined. Ammonium sulfate was added to 50% saturation, and the solution stirred for about 1 h. The precipitate was centrifuged and redissolved with gentle shaking in 10 mL of 50 mM potassium phosphate buffer (pH 7.5), containing 0.001% Triton X-100. The sample was then centrifuged to remove any undissolved particulates, filtered through a 0.8 μm sterile filter, and applied to a 26/60 Hiload Superdex 75 prep grade gel filtration column (Pharmacia) at a flow rate of 2.5 mL/min. The active fractions were pooled, concentrated, and dialyzed against a buffer containing 100 mM potassium phosphate and 500 mM ammonium sulfate. This sample was then applied to a hydrophobic interaction column (Phenyl Superose HR10/10, Pharmacia) previously equilibrated with the same buffer. The column was washed with starting buffer until the baseline had returned to zero and was then eluted with 50 mM potassium phosphate (pH 7.5), containing no ammonium sulfate at a flow rate of 0.5 mL/min. The single peak was concentrated and found to be greater than 95% pure by SDS−PAGE. Typical yields of pure PHMcc were about 50 mg, starting from 7 days of bioreactor harvest.

PHM Mutants. Cell lines carrying specific site mutations of PHMcc (M314I and H242A) were constructed and kindly provided to us by Drs. Aparna S. Kolhekar, Richard E. Mains, and Betty A. Eipper. Full details of the construction and properties of these mutants have been reported previously (*16*, *18*).

Copper Reconstitution. As isolated, PHM contained only ~0.3 Cu/protein. Following purification, the protein was dialyzed for 2 days in 0.05 M potassium phosphate containing 25 μM Cu^{2+} as $Cu(NO_3)_2$, with a change of buffer after day 1. Following this procedure, the Cu/protein ratio was typically in the range 1.5−2.1. The CO:Cu binding ratio of the fully reduced protein (see below) was found to be the best index of homogeneous loading of the copper centers and the absence of adventitiously bound copper. A value for CO:Cu of 0.5 indicated homogeneous reconstitution.

Copper and Protein Concentration. Protein concentration was initially determined using the Bicinchoninic Acid Protein Assay Kit (Sigma). The extinction coefficient ($A_{0.1\%}$, 280 nm) was then calculated, and the average of five experiments was found to be 0.98. Thereafter, the OD_{280} was used to determine protein concentration. OD_{280} measurements were recorded on a Shimadzu UV-268 spectrophotometer at ambient temperature. Copper concentrations were determined by flame atomic absorption on a Varian-Techtron AA5 spectrometer against standard copper solutions spanning the range 5−20 μM; all protein samples were diluted to be within this range. In most cases, protein and copper analyses were performed on the same 1 mL sample of enzyme, which eliminated dilution errors from the determination of copper-to-protein ratios.

Activity Measurements. Enzyme activity was determined from the rate of oxygen consumption using a Rank Brothers oxygen electrode at 37 °C. The following reagents were added to a stirred cell and were allowed to equilibrate until a flat baseline was obtained. Mes, 1660 μL of 150 mM; Cu^{2+}, 100 μL of 100 mM; catalase, 200 μL of 130 000 units/mL stock solution; ascorbate, 10 μL of 220 mM; PHM, 10 μL of 0.3−1.5 mg/mL solution. The cell was fitted with a Lucite stopper with a minimal opening to prevent oxygen from the air entering the solution. The reaction was initiated with 20 μL of 25 mM peptide substrate N-Ac-tyr-val-gly (N-AcYVG) and was allowed to run until completion (around 3 min). The slope of the line was used to calculate activity, defined as micromoles of O_2 consumed per minute per milligram of enzyme, using a value of 178 μM for the concentration of oxygen in air-saturated buffer at 37 °C (Handbook of Physical Chemistry). Activities of preparations used in this study varied between 15 and 20 units/mg.

Measurement of CO Binding Stoichiometry. A modification of the protocol described by Reedy et al. (*20*) was used to measure the stoichiometry of CO binding to the copper centers in PHMcc. Sixty microliters of a concentrated PHM sample (at least 800 μM in Cu) was transferred to an airtight conical vial. An equal volume of buffer was transferred to a second airtight conical vial. Both samples were made anaerobic by vacuum flushing with Ar, and a 5-fold excess of ascorbate was added to reduce the copper centers. Both vials were connected via a T-piece to a single gas line and equilibrated with the same partial pressure of CO (~1 atm). A 50 μL sample of the carbonylated enzyme was removed for infrared analysis.

A small volume (5.5 μL) of hemoglobin (~3.4 mM in Fe sites) was made anaerobic in a serum vial by repeated vacuum flushing with Ar. To this were added 3 μL of anaerobic buffer (50 mM potassium phosphate, pH 7.5) and 2 μL of ascorbate oxidase (1 unit/μL in 50 mM potassium phosphate, pH 7.5). The mixture was gently vacuum flushed until it darkened slightly. Two microliters of anaerobic ascorbate (330 mM in 100 mM sodium acetate, pH 6.0) was added with continued Ar flushing. After 15 min, an additional 2 μL of ascorbate was added with vacuum flushing, and the mixture was left under Ar for 20 min. A 2 mm path-length quartz cuvette fitted with an airtight septum was vacuum flushed with Ar, and 700 μL of anaerobic acetate buffer (100 mM, pH 6.0) was added. This solution was used to zero the baseline of the UV−vis spectrophotometer. After the baseline was recorded, 5 μL of ascorbate (330 mM in acetate buffer, pH 6) and 5 μL of ascorbate oxidase (1 units/mL in 50 mM potassium phosphate, pH 7.5) were added, and the cell was inverted 10 times. An aliquot (4 μL) of the hemoglobin solution was added to the cell, the cell was inverted to mix the reagents, and a visible spectrum was recorded from 400 to 460 nm. The spectrum was rerecorded every 20 min until the absorbances at 419 nm (Hb-O_2 and Hb-CO) and 430 nm (deoxyHb) remained constant. This procedure ensured complete deoxygenation of the hemoglobin solution.

CO-saturated buffer was titrated into the deoxyhemoglobin solution in aliquots of 0.6 μL, and the absorbance at 419 nm was recorded. The change in absorbance (ΔA_{419}) was plotted against the total volume of CO-saturated buffer added. The $[CO]_{buffer}$ was calculated using the equation

$$[CO]_{buffer} = (SV)/(\Delta\epsilon_{419}l)$$

where S is the slope of the plot of ΔA_{419} vs aliquots of CO added, V is the total volume in the cuvette at the end of the titration, $\Delta\epsilon_{419}$ is the difference between the extinction coefficients of carbonmonoxy- and deoxy-hemoglobin at 419 nm, and l is the path length of the cuvette. The titration was continued using 0.6 μL aliquots from the PHM−CO reaction mixture, and the $[CO]_{PHM+buffer}$ was calculated similarly. The difference between $[CO]_{PHM+buffer}$ and $[CO]_{buffer}$ gave the concentration of CO bound to the enzyme. An aliquot of the PHM−CO reaction mixture was then analyzed for copper content, allowing the [CO]/[Cu] binding ratio to be determined.

CO Binding to PHM in the Presence of Substrate. A 2-fold excess of substrate (N-AcYVG or hippuric acid) was added to 40 μL of PHMcc in a conical vial. The solution was made anaerobic by repeated vacuum flushing with Ar and left under 1−1.5 atm of Ar for 15 min. A 5-fold excess of ascorbate was then added with additional flushing of Ar. The vial was vacuum flushed with CO three times and was left under a constant pressure of CO for at least 20 min. Samples for IR, XAS, and stoichiometry measurements were prepared from the product.

Isotope Shifts and Reversibility of CO Binding. A sample of PHMcc (800 μM) was made anaerobic in a 1 mL conical vial fitted with a septum and then reduced with a 5-fold excess of ascorbate. A 2.5 mL volume of ^{13}CO gas was injected via gastight syringe into the vial (to increase the p_{co} to approximately 2−2.5 atm), and the PHM−CO reaction mixture was allowed to equilibrate on ice for 20 min, after

which its IR spectrum was recorded. The sample was then flushed with ^{12}CO at ambient pressure, and the IR spectrum was again recorded. The experiment was repeated in the presence of a 2-fold excess of N-AcYVG or 10 mM hippuric acid.

Titration of PHM with N-AcYVG and Subsequent Carbonylation. A sample of oxidized PHM, with an initial concentration of 1.6 mM, was separated into 5 aliquots of 40 μL each. Each portion of enzyme received an increasing number of mole equivalents N-AcYVG peptide substrate (0.0, 0.1, 0.5, 1.0, and 5.0 equiv, respectively). Each mixture was then sealed with a septum in a separate vial and made anaerobic by vacuum flushing with Ar. After anaerobiosis was achieved, the enzyme was reduced with a 5-fold excess of anaerobic ascorbate, and the PHM−substrate adduct was exposed to pure CO by vacuum flushing. Each vial was left under a pressure of CO for at least 20 min. (This time was determined previously to be sufficient for full carbonylation of small volumes of concentrated enzyme.) For each sample, 35 μL was transferred anaerobically to an infrared cell for IR analysis.

IR Spectroscopy. Solution IR spectra were recorded on a Perkin-Elmer System 2000 FTIR with a liquid nitrogen-cooled mercury cadmium telluride detector. Protein solutions were injected into a 0.050 cm path-length transmission IR cell fitted with CaF_2 windows and placed in a constant humidity sample compartment that was kept at 10 °C. Samples were kept at 10 °C to inhibit formation of bubbles from the outgassing of carbon monoxide during infrared irradiation of the sample. Two hundred scans were collected for each sample, and the compilation and analysis of spectra were performed using the Perkin-Elmer program Spectrum for Windows. An initial spectrum (200 scans) of the empty chamber was taken and used as the background which was subtracted automatically by the program from each subsequent spectrum. To remove the large water band at 2140 cm^{-1}, 200 scans of deionized water were averaged and then manually subtracted from the protein spectra. Water background subtraction was completed using the interactive polynomial baseline subtraction routine of the Spectrum program.

X-ray Absorption (XAS) Data Collection and Analysis. XAS data for the CO complex of PHM were collected at the Stanford Synchrotron Radiation Laboratory (SSRL) on beam line 7.3, operating at 3.0 GeV with beam currents between 100 and 50 mA. A Si220 monochromator with 1.2 mm slits was used to provide monochromatic radiation in the 8.8−10 keV energy range. The monochromator was detuned 50% to reject harmonics. The protein samples were measured as frozen glasses in 21% glycerol at 11−14 K in fluorescence mode using a 13-element Ge detector. To avoid detector saturation, the count rate of each detector channel was kept below 100 kHz by adjusting the hutch entrance slits or by moving the detector in or out from the cryostat windows. Under these conditions, no dead-time correction was necessary. The summed data for each detector was then inspected, and only those channels that gave high quality backgrounds free from glitches, drop outs, or scatter peaks were included in the final average. Twelve 35 min scans were collected for the PHM−CO complex.

Raw data were averaged, background subtracted, and normalized to the smoothly varying background atomic absorption using the EXAFS data reduction package EXAFSPAK (*24*). Energy calibration was achieved by reference to the first inflection point of a copper foil (8980.3 eV) placed between the second and third ion chambers. In any series of scans, the measured energy of the first inflection of the copper foil spectrum varied by less than 1 eV. Averaged EXAFS data were referenced to the copper calibration of the first scan of a series, since the energy drift in any series of scans was too small to perturb the EXAFS oscillations.

Table 1: Stoichiometry of Carbon Monoxide Binding to Reduced PHMcc

	$[CO]_{sample}$ (mM)	$[CO]_{buffer}$ (mM)	$[CO]_{bound}$ (mM)	[Cu] (mM)	[CO]/[Cu]
WT 3/97	1.40	1.08	0.31	0.57	0.54
4/97	1.42	0.84	0.58	1.24	0.46
DβM[b]	2.79	2.10	0.70	1.38	0.50
PAM[c]					0.52
H242A[a]					
1/98	1.08	1.18	0	1.00	0
06/98	0.83	0.71	0	0.83	0

[a] This work. [b] From ref *23*. [c] From ref *15*.

Data analysis was carried out by the least-squares curve-fitting program EXCURV98 which utilizes full curved-wave calculations as described by Gurman and co-workers (*25*−*28*). The application to metalloprotein systems, particularly the treatment of imidazole rings from histidine residues, and of linearly coordinated carbonyl groups by multiple scattering analysis has been described in detail in previous papers from this laboratory (*23*, *29*−*31*). The parameters refined in the fit were as follows: E_0, the photoelectron energy threshold; R_i, the distance from Cu to atom i; and $2\sigma^2_i$, the Debye−Waller (DW) term for atom i. In general, coordination numbers were fixed at values consistent with the crystallographic description of PHMcc and the measurements of CO binding stoichiometry, but were allowed to float in some fits to test the consistency between spectroscopic, biochemical, and crystallographic results. In the latter case, the coordination numbers were constrained to produce DW factors within reasonable limits (first shell, $0 < 2\sigma^2 < 0.015$; second shell ≥ first shell). The goodness of fit was judged by reference to a goodness of fit parameter, F, defined as

$$F^2 = \frac{1}{N}\sum_{i=1}^{n} k^6(\text{data}_i - \text{model}_i)^2$$

RESULTS

Stoichiometry of CO Binding to Wild-Type PHM. Purified wild-type (wt) PHMcc was found to contain ≤0.3 Cu/protein. Therefore, it was necessary to reconstitute the enzyme with copper as described in the Experimental Procedures. For enzyme samples used in the present work, this protocol produced enzyme with 1.3−2.1 coppers bound/molecule of PHMcc. The stoichiometry of CO binding to reduced PHMcc was determined using these reconstituted protein samples. Results from four separate experiments showed that one molecule of CO binds per two active-site coppers, with a calculated average of 0.50 CO/Cu. Data from two representative experiments are shown in Table 1. These results are comparable to previous results for DβM and PAM, which were also found to bind 0.5 mole equivalents of CO per Cu(I) (*15*, *22*). It is thus clear that, like DβM and PAM, the

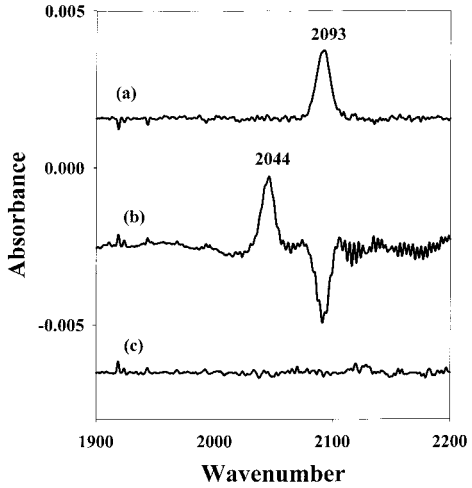

FIGURE 2: Fourier transform infrared spectra of the complexes formed in the reaction of carbon monoxide with reduced PHMcc and a H242A site-directed mutant. (a) CO complex of wt reduced enzyme. (b) ^{13}CO minus ^{12}CO difference spectrum for the wtPHM−CO complex: the ^{12}CO spectrum was generated by vacuum flushing of the PHM−^{13}CO complex with natural abundance CO gas. (c) FTIR spectrum of the reduced H242A mutant reacted with CO using identical conditions as in panel a.

Table 2: Infrared Frequencies and Isotope Shifts for Carbonyl Complexes of PHMcc and Other Copper Proteins

protein	^{12}CO	^{13}CO	$\Delta\nu$(CO)	ref
PHM[a]	2093	2044	−49	this work
PHM + AcYVG[a]	2093	2044	−49	this work
	2062	2016	−46	
PHM + hippuric acid[a]	2093	2044	−49	this work
	2075	2028	−47	
DβM[b]	2089			*23*
PAM[c]	2093			*16*
Hc[d]				
molluscan	2063	2017	−46	*32*
limulus	2053	2007	−47	*32*
arthropodal	2043			*32*
cytochrome oxidase[e]				
aa_3	2062			*33*
bo_3	2065			*36*

two copper centers in PHMcc are inequivalent with respect to reactivity toward carbon monoxide.

Infrared Analysis of CO Binding to wtPHM. Figure 2a shows the Fourier transform infrared (FTIR) spectrum of CO-bound wtPHMcc. A single, strong, infrared frequency is observed at ν(CO) = 2093 cm^{-1} assignable to the PHMcc−carbonyl complex. This value is reported in Table 2 along with ν(CO) values for other carbonyl complexes of copper proteins including bifunctional PAM, DβM, hemocyanin (Hc), and cytochrome *c* oxidase (CCO) for comparison. The infrared band for PHMcc is close to the published value of ν(CO) = 2089 cm^{-1} for DβM−CO, which was assigned as the C−O stretching frequency for CO bound at the Cu_B (methionine ligated) center. The IR frequencies for molluscan Hc (*32*) and CCO (*33*−*36*) are 2063 and 2062 cm^{-1}, respectively, 20 cm^{-1} lower than the Cu-carbonyls of PHM or DβM.

^{13}CO Isotope Binding Data. The results of the binding of isotopically labeled ^{13}CO to wtPHMcc are shown in Figure 2b and Table 2. The FTIR spectrum of the ^{13}CO-treated enzyme shows a single band at 2044 cm^{-1}, which represents an isotope shift of 49 cm^{-1}, close to the expected isotope shift of 47 cm^{-1} for a linearly coordinated CO molecule. This allows definitive assignment of the peak as a carbonyl. When the PHM−^{13}CO sample was flushed with ^{12}CO, the 2044 cm^{-1} peak was replaced by the 2093 cm^{-1} peak, as shown by the difference spectrum (^{13}CO−^{12}CO) in Figure 2b. This is good evidence that CO binding to PHM is completely reversible. Similar isotope frequency shifts are found in other Cu(I)-carbonyl adducts (Table 2). For example, the ν(CO) for Hc downshifts 46 cm^{-1} when CO is replaced with ^{13}CO.

Copper Binding, CO Stoichiometry, and Infrared Spectroscopy of the H242A Mutant. Our data show that PHMcc binds CO at only one copper center, and comparison to previously published data on native DβM (*20*, *23*) suggests that the binding occurs at the methionine-containing Cu_B center. Therefore, we examined the stoichiometry and IR spectroscopy of CO binding to a mutant which was expected to lack the Cu_B center. M314, H242, and H244 are the three endogenous ligands to Cu_B, and mutation of any one of these to a noncoordinating residue such as isoleucine or alanine would be expected to disrupt copper binding to the site. Unpublished work from our laboratory has shown that the M314I mutant is probably unable to form the Cu_B center and that it has an unusual EXAFS spectrum indicative of a 2-coordinate, all histidine copper center (Cu_A) in its reduced form. However, this mutant still appeared to bind low levels of CO ($\leq$0.2 CO/Cu) with a similar frequency to wtPHMcc, suggesting that the Cu_B center may still be able to form in the presence of CO. To overcome this ambiguity, we have investigated CO binding to the H242A mutant. The EXAFS spectrum of the reduced H242A derivative (unpublished data) is identical to that of the reduced M314I derivative with no contribution from the S(M314), which establishes unambiguously that the Cu_B center has been disrupted. Following identical protocols used for total copper reconstitution in wtPHM, the mutant H242A was found to bind only one copper per protein, confirming that one of the copper centers has been lost. The single copper in the H242A mutant was unable to bind carbon monoxide. Data from two separate CO binding experiments are presented in Table 1, and the FTIR spectrum (measured under identical experimental conditions to wtPHMcc) is shown in Figure 2c. These data support the premise that the binding of CO takes place at the Cu_B site in PHM.

XAS of PHM−CO. EXAFS data for a sample of the PHM−CO complex (0.50 CO/Cu) are shown in Figure 3. The Fourier transform shows a well-resolved splitting of the first shell due to the presence of short ($\sim$1.8−2.0 Å) Cu−C(CO) and Cu−N(imid) interactions and the longer (2.3 Å) Cu−S(methionine) interaction. Since the crystal structure has defined the ligand set at each of the copper centers and the stoichiometry measurement shows that CO binds to only one of the two copper centers (Cu_B), meaningful simulation of the EXAFS data can only be achieved by using a two-site model which treats each copper center separately. Our simulation method thus allowed the imidazole shells (single and multiple scattering) associated with each copper to refine independently, together with the contributions from 0.5 CO and 0.5 S(methionine) ligands. The best fit obtained is shown in Figure 3 with metrical parameters listed in Table 3.

The EXAFS simulations give Cu−C(CO) and Cu−S(met) distances of 1.82 ± 0.03 and 2.33 ± 0.01 Å, respectively,

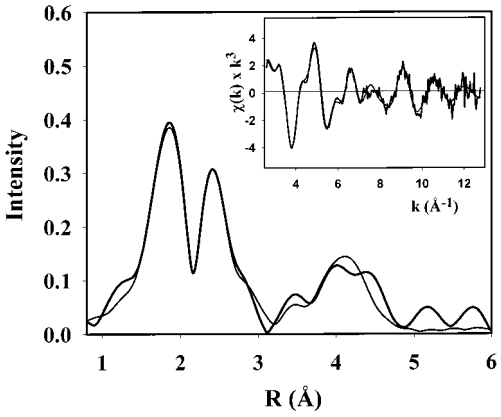

FIGURE 3: Fourier transform and EXAFS (inset) of reduced wtPHMcc reacted with carbon monoxide. Solid thick lines represent the experimental data; solid thin lines represent the simulated data. Parameters used to generate the fit to the EXAFS data are listed in Table 3.

and show the presence of two distinct populations of Cu−imidazole interactions at 1.90 ± 0.01 and 2.01 ± 0.01 Å, respectively. Although this splitting is at the limit of the resolution of the data ($\Delta R = \pi/2\Delta k = 0.11$ Å), it is consistent with one 2- or 3-coordinate center (Cu_A) with histidine-only coordination [Cu−N(imid) 1.90 Å] and one 4-coordinate copper center (Cu_B) with two histidines (2.01 Å), methionine-S (2.33 Å), and CO (1.82 Å). The Cu−S(met) distance is 0.10 ± 0.02 Å longer than found in uncarbonylated reduced enzyme, which is consistent with replacement of a weakly bound coordinated solvent with the stronger-field carbonyl ligand and provides strong evidence that the CO is bound at the methionine site. The Cu−CO distance of 1.82 Å is in the range expected for a Cu(I)-carbonyl (*37*−*41*). Interestingly, no multiple scattering is detected from the supposedly linear Cu−C−O triatom unit, perhaps suggesting a statically disordered orientation for the CO group.

CO Binding to PHMcc in the Presence of Substrate. The stoichiometry of CO binding to PHMcc in the presence of the peptide substrate N-AcYVG was determined, and the results are shown in Table 4. These data show that the CO binding stoichiometry for peptide-bound wtPHM increases from 0.5:1 to close to 1:1. Comparison with the data in Table 1 shows that the increase of CO bound per copper appears as an increase in the concentration of CO complexed in the aqueous PHM−CO sample, rather than a decrease in the copper concentration. Four individual experiments were run on four distinct preparations of PHM, and the average ratio for the stoichiometry was found to be 0.85. This strongly suggests that binding of peptide to reduced PHM activates a second site for CO binding which may be at the second copper center (Cu_A).

Infrared Spectra and Isotope Shifts for CO Binding to PHMcc in the Presence of Substrate. The infrared spectrum of N-AcYVG-bound PHM + CO is shown in Figure 4a. A second IR band at a frequency of 2062 cm^{-1} is reproducibly observed along with the original carbonyl stretching frequency at $\nu(CO) = 2093$ cm^{-1}. ^{13}CO isotope labeling studies show a shift in each band of −46 and −49 cm^{-1}, respectively, which revert back to the original frequencies upon flushing with naturally abundant CO (Figure 4b). When the alternative substrate hippuric acid (benzoylglycine) was used instead of N-AcYVG, the second band shifted to 2075 cm^{-1} with an isotope shift of −47 cm^{-1} (Figure 4, panels c and d). The isotope shifts conclusively assign the substrate-induced frequencies as copper−carbonyls and show that the binding is completely reversible.

Two possibilities exist to explain the origin of the second CO band. Substrate binding could perturb the copper coordination at Cu_B such that the CO frequency was itself perturbed. In this case, we would expect that, at the high substrate concentrations used here (2 orders of magnitude above the K_m), the 2093 cm^{-1} band would be completely converted into the 2062 cm^{-1} band, as the resting state was completely converted into the substrate activated form. On the other hand, if the second CO band arises from CO binding at a second site, then we would expect the 2093 and 2062 cm^{-1} bands to coexist even at high substrate concentrations. The CO binding stoichiometry argues in favor of the latter. However, as a more stringent test, we undertook an IR titration of the enzyme under a CO atmosphere with up to a 5-fold excess of substrate. The results are shown in Figure 5. The 2062 cm^{-1} band grows in and maximizes with no loss in intensity of the 2093 cm^{-1} band, indicating that the 2062 cm^{-1} band must arise from binding of CO at a second site.

DISCUSSION

The activation of dioxygen by copper monooxygenases has been studied for over three decades. Crystallographic studies on hemocyanin (*42*−*44*) and catechol oxidase (*45*) have provided a clear picture of the way that dioxygen binds and is activated in dinuclear active sites. For example, in hemocyanins, the two copper atoms are each ligated by three histidine residues and are separated by 3.5−4 Å. This configuration allows the O_2 molecule to bridge in a $\eta_2-\eta_2$ (side-on) fashion and to accept one electron from each copper to form coordinated peroxide. In contrast to these dinuclear systems, PHM and DβM contain mononuclear, chemically inequivalent copper centers separated by 11 Å. Comparison of the X-ray crystal structure (oxidized enzyme) with EXAFS results (oxidized and reduced forms) has revealed the catalytic copper centers in considerable detail (*15*, *19*). The Cu_A center is coordinated by three histidines (H107, H108, and H172) via their Nδ nitrogens in what appears to be T-shaped geometry. More recent EXAFS analysis of the reduced enzyme (unpublished data) supports a model in which the H107 and H108 residues are approximately trans to each other with short (1.88 Å) Cu−N bonds and no detectable interaction with H172. Cu_B is ligated by two histidines (H242 and H244) and a methionine (M314) with some evidence for a fourth solvent ligand. Since these centers differ by the substitution of one histidine at Cu_B for a methionine, for clarity, we will refer to the Cu_A center as the histidine site and the Cu_B center as the methionine site. A crystal structure of the oxidized enzyme soaked with diiodotyrosylglycine shows that this substrate binds with its carboxylate group salt-bridged to the guanidinium group of R240 and with a further H-bond to the hydroxyl of Y318, such that the peptide is oriented toward the methionine site. In this conformation, the C_α of the substrate is nicely aligned to interact with a peroxide located at the solvent-accessible coordination position on Cu_B.

A crucial mechanistic question is how such an intermediate could be formed. The 11 Å intermetal distance precludes

Table 3: Parameters Used to Simulate the EXAFS and Fourier Transform of Reduced Carbonylated PHMcc (PHM−CO)

first shell[a]			outer shells[a]			
shell (*X*)	*R* (Å)	$2\sigma^2$(Å^2)	shell (*Y*)	*R* (Å)	∠Cu−X−Y (deg)	$2\sigma^2$ (Å^2)
			$F = 0.776$, $E_0 = -1.90$ eV			
0.5 C (CO)	1.82	0.003	0.5 O (CO)	2.85	179	>0.05
1 N_α (imid A)	1.90	0.006	1 C_β (imid)	2.90	128	0.007
			1 C_β (imid)	2.82	235	0.007
			1 C_γ/N_γ (imid)	4.08	197	0.012
			1 C_γ/N_γ (imid)	4.15	162	0.012
1 N_α (imid B)	2.01	0.007	1 C_β (imid)	2.96	236	0.008
			1 C_β (imid)	3.02	128	0.008
			1 C_γ/N_γ (imid)	4.22	201	0.012
			1 C_γ/N_γ (imid)	4.29	164	0.012
0.5 S (M314)	2.34	0.009				

[a] Estimated errors in distances are ±0.01 Å for the first shell and ±0.03 Å for outer shells except for the Cu−C(CO) distance where the error is ±0.03 Å. Estimated errors in coordination numbers are ±25%. ∠Cu−X−Y (deg) represents the angle between the first shell scatterer (*X*) and the outer shell scatterer (*Y*). Estimated errors in angles are ±5° except for the ∠Cu−C−O where the high Debye−Waller term for the carbonyl O atom precludes precise determination.

Table 4: Stoichiometry of Carbon Monoxide Binding to wtPHMcc in the Presence of the Peptide Substrate N-AcYVG

preparation	$[CO]_{PHM+buffer}$ (mM)	$[CO]_{buffer}$ (mM)	$[CO]_{PHM}$ (mM)	$[Cu]_{PHM}$ (mM)	[CO]/[Cu]
A	1.68	0.93	0.75	0.92	0.80
B	1.29	0.96	0.33	0.55	0.59
C	1.62	0.47	1.15	1.29	0.89
D	2.23	0.76	1.47	1.31	1.13
average					0.85

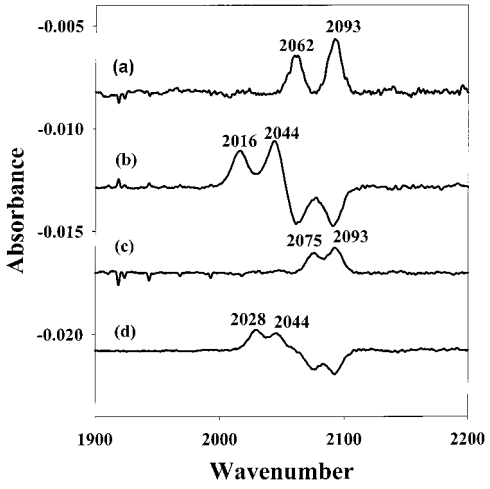

FIGURE 4: Fourier transform infrared spectra of the complexes formed in the reaction of carbon monoxide with reduced PHMcc in the presence of substrates. (a) CO complex of wt reduced enzyme + 2 molar equivalents N−AcYVG. (b) ^{13}CO minus ^{12}CO difference spectrum for the wtPHM−CO complex + N-AcYVG; the ^{12}CO spectrum was generated by vacuum flushing of the PHM−^{13}CO complex with natural abundance CO gas. (c) CO complex of wt reduced enzyme + 10 mM hippuric acid. (d) ^{13}CO minus ^{12}CO difference spectrum for the wtPHM−CO complex + 10 mM hippuric acid; the ^{12}CO spectrum was generated by vacuum flushing of the PHM−^{13}CO complex with natural abundance CO gas.

any kind of dioxygen bridge which might facilitate direct electron transfer from each Cu(I) to O_2. One alternative is for O_2 to bind at one of the Cu(I) centers forming a Cu(II)−superoxo complex and for the second electron necessary to complete the formation of peroxide to arrive via long-range electron transfer. Previous studies from this laboratory used CO binding to probe potential binding sites for O_2 in

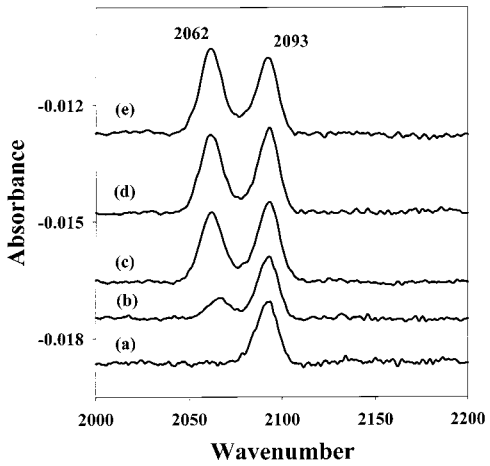

FIGURE 5: Titration of the PHM−CO complex with increasing amounts of N-AcYVG substrate. (a) 0 equiv substrate; (b) 0.1 equiv; (c) 0.5 equiv; (d) 1.0 equiv; (e) 5.0 equiv.

the related PAM and DβM enzymes and concluded that the methionine (Cu_B) locus was the site of CO/O_2 binding, based on the following evidence (*15*, *20*, *22*, *23*). First, both enzymes bound only 0.5 CO/copper, indicating that CO bound at only one of the two coppers. Second, a single intraligand CO stretching frequency was observed in the FTIR spectra at 2093 and 2089 cm^{-1} for PAM and DβM, respectively, a frequency which was more consistent with the His-His-Met ligand set at Cu_B than the $(His)_3$ ligand set at Cu_A. Third, we were able to prepare a Cu_A-depleted derivative of DβM which was shown to retain both the S scattering contribution from the methionine in the EXAFS and the CO binding activity (1 CO/Cu).

On the basis of their crystal structure, Prigge and co-workers also proposed that dioxygen binds to the methionine site and is converted to peroxide via a long-range ET event. However, since the copper centers are located in different domains and the structure reveals no through-bond ET pathway shorter than ~50 Å, they were forced to propose that electron transfer occurs through the intervening solvent (but see note added in proof). As discussed by Gray and Winkler (*21*), long-range ET rates are strongly dependent on the medium, being greatest for β-structure and significantly less for α-helices. The efficiency of ET through H-bonded networks of *ordered* water molecules appears to

be roughly equivalent to the lower limit for α-helices, predicting maximum k_{ET} values of $<10^6$ s^{-1} for a donor−acceptor distance of 11 Å (H. B. Gray, personal communication). The fastest step in the PHM mechanism (with hippuric acid as substrate) has been estimated by Klinman and co-workers to be the decomposition of ESO_2 with a first-order rate constant of 810 ± 120 s^{-1} (*11*). Thus, solvent-mediated ET could be consistent with the observed reaction rates, provided that the solvent provided an ordered network of H-bonds connecting the two copper centers.

Two other factors are likely to dramatically reduce the ET rates in the PHM system. First, the different coordination geometries preferred by Cu(II) and Cu(I) often impose severe Frank Condon restrictions on ET rates; second, the reorganizational energies inherent in ET between solvated metal ions embedded in bulk solvent are also likely to lead to slower reactions. Although no data are available on electron-transfer rates in systems comparable to PHM, some insights can be obtained from comparisons of self-exchange rates of Cu(II/I) redox couples.

Cu(II/I) self-exchange rates span a wide range of values (*46*, and references therein). Among the fastest are the k_{11} values for cupredoxins which lie between 10^5 and 10^3 M^{-1} s^{-1} with associated k_{ET} values around 10^6 s^{-1} (*46*, *47*). These rapid rates are generally attributed to low reorganizational energies resulting from an "entatic" state, i.e., a strained geometry around the copper center which lies midway between the preferred coordination geometries of cupric (tetragonal or square) and cuprous (tetrahedral or trigonal) sites (*48*). Inorganic complexes containing macrocyclic ligands which constrain the amount of structural change possible during redox also lead to fairly rapid self-exchange rates in the range 10^3-10^5 M^{-1} s^{-1} (*49*−*51*). Stanbury and co-workers (*46*) have undertaken a quantitative analysis of the internal structural reorganizational energy and the solvent reorganizational energy that accompanies redox and have correctly predicted differences between self-exchange rates. For example, although k_{11} values for the couples [Cu(II/I)-$(bib)_2$] [bib = 2,2′-bis(2-imidazolyl)biphenyl] and [Cu(II/I)-$(bimdpk)_2$] [bimdpk = bis(1-methyl-4,5-diphenylimidazol-2-yl)ketone] are 0.16 and 1.9×10^4 M^{-1} s^{-1}, respectively, differing by 5 orders of magnitude, molecular dynamics calculations show convincingly that this difference can be traced to the much greater angular distortions that accompany redox reactivity of the [Cu(II/I)$(bib)_2$] system. For systems involving large changes in both structure and coordination number, dramatically slower self-exchange rates are observed, for example [Cu(II/I)(aq)], 5×10^{-7} M^{-1} s^{-1}, and [Cu(II/I)$(Im)_n$], 1×10^{-7} M^{-1} s^{-1} (*52*). These studies provide a quantitative basis for the premise that ET rates in copper complexes depend critically on the extent of structural and solvent reorganization, which accompanies the redox process and will be slow in cases involving large angular distortions or changes in coordination number.

As discussed above, our XAS data have provided evidence for significant structural change at both copper centers in PHM during redox. The Cu_A center changes from 4- or 5-coordinate tetragonal to highly distorted (T-shaped) trigonal with an estimated 0.3−0.5-Å movement of a histidine ligand (H172). The Cu_B center changes from 4- or 5-coordinate tetragonal to trigonal or tetrahedral coordination, with an estimated 0.5 Å movement of the M314 ligand. In addition, whereas the model complexes discussed above are presumed to form an outer-sphere donor−acceptor complex in which the coordination spheres of each complex touch in the transition state [with center-to-center distances of <8 Å (*49*], the coordination spheres of each copper center in PHM are constrained to remain separated by 11 Å during the ET event. These structural elements all point to the conclusion that solvent-mediated ET between the copper centers of PHM is likely to be extremely slow, and other mechanisms for the formation of the Cu_B-OOH reactive intermediate should be considered.

The present work has used CO to probe the chemistry of dioxygen interaction with the copper centers of PHMcc. The results indicate a stoichiometry of 0.5 CO/Cu and a single band in the FTIR spectrum [ν(CO) = 2093 cm^{-1}]. Thus, they parallel the earlier work on PAM and Dβ M and establish that PHMcc also binds a single CO at the methionine site. Isotope substitution with ^{13}CO confirms that the 2093 cm^{-1} band is a Cu-carbonyl, while the facile exchange of ^{13}CO with ^{12}CO indicates that binding is reversible. Two other pieces of evidence provide confirmation of the assignment. First, a His242 to Ala site-directed mutant (which lacks the ability to bind copper at the methionine site) is unable to bind CO and has no IR band in the 1950−2300 cm^{-1} region. Second, binding of CO to wtPHMcc causes a 0.10 ± 0.02 Å increase in the Cu−S(met) bond length, which is consistent with replacement of a weakly coordinating solvent by a strong field ligand such as CO at the Cu_B center. These results provide unambiguous evidence that, in the absence of substrate, a single CO binds to the methionine site.

How can this result be reconciled with the unfavorable nature of ET through solvent? The answer may lie in the additional CO binding site observed in the presence of peptide substrates. When 1 equiv of N-AcYVG is added to the CO binding assay, the CO:Cu ratio increases toward 1 (average of 0.85), and a second FTIR band appears at 2062 cm^{-1}. The 2062 cm^{-1} band titrates with the added substrate without loss in intensity of the 2093 cm^{-1} band. ^{13}CO substitution induces a 49 cm^{-1} downshift, indicative of a coordinated carbonyl, while facile exchange with ^{12}CO establishes reversibility. This new band thus has all the properties of a Cu-carbonyl. The fact that its formation affects neither the frequency nor the intensity of the Cu_B−CO adduct proves that it must bind at a site other than Cu_B. Hence, we propose that the 2062 cm^{-1} band arises from substrate-induced binding of CO at the Cu_A (histidine) site. Of particular interest is the observation that ν(CO) is dependent on the nature of the bound substrate, since with hippuric acid (benzoylglycine) the band is found at 2075 cm^{-1}, 13 cm^{-1} above that of N-AcYVG.

The observed frequency of the second Cu−CO is 20−30 cm^{-1} lower than that for the Cu_B-carbonyl. The lower frequency is entirely consistent with the proposed Cu$(His)_3$CO coordination. Histidine is a stronger donor than methionine, and the additional electron donation allows more back-bonding from Cu(I) to CO, thus lowering the frequency. The extensive literature of structurally characterized Cu(I) carbonyls makes it possible to further quantify this correlation between IR frequency and ligand donor set/coordination number (*22*, *37*, *39*). Four-coordinate complexes with N_3-

CO donor atom sets typically absorb in the range 2065−2085 cm^{-1}, while three coordinate N_2CO complexes absorb above 2090 cm^{-1}. Thus, the 2093 cm^{-1} Cu_B−CO adduct obeys the correlation if we assume that the thioether S atom is essentially neutral with respect to its electron-donating power, while the 2062 cm^{-1} band is at the lower end of the range expected for a N_3CO donor atom set. It should be noted that the Cu(I)−CO complexes of other proteins with Cu-$(His)_3$ active sites, such as molluscan hemocyanin and cytochrome *c* oxidase, absorb at the same frequency (2062 cm^{-1}) as the Ac-YVG-induced PHM−CO complex (*32*−*36*).

The discovery that substrate binding turns on CO- and (by inference) O_2-binding activity at the Cu_A center in PHM has allowed us to suggest a completely new mechanism for oxygen activation and formation of the reactive peroxo intermediate as shown in Figure 6. We propose that in the resting enzyme, the Cu_A site is unreactive to either CO or O_2. Substrate binding induces a structural or electronic perturbation at Cu_A, which turns on its O_2 reactivity and results in the initial formation of a Cu_A(II)-$O_2^{\bullet}$ intermediate. Such a step would be entirely consistent with a recent finding that the mechanism is equilibrium ordered with substrate binding first (*11*). The superoxide next dissociates from the Cu_A, either as a solvated anionic species or it picks up a proton and dissociates as the neutral $HO_2^{\bullet}$. It then diffuses across the 11 Å solvent channel where it reacts with the reduced $Cu(I)_B$ center, forming the proposed Cu_B-hydroperoxo intermediate. In this mechanism, the extra electron and possibly also the proton required to form the hydroperoxo intermediate would be carried by the oxygen substrate itself rather than via a protein-based ET pathway.

A problem that remains is how the enzyme prevents diffusion of superoxide out of the channel, with the resulting uncoupling of dioxygen reduction and substrate hydroxylation. At present, this remains an open question, but a number of possible scenarios exist that could circumvent superoxide leakage. One possibility is that Y79, located 4 Å from Cu_A (Figure 6), could H-bond to the superoxide anion, providing an assisted channeling pathway. A second option is that dioxygen might bind at both copper centers, generating a Cu(II)-superoxo species at each. The superoxide formed at Cu_A might then channel, assisted by H-bonding to Y79, and undergo a dismutation reaction with the superoxide bound at Cu_B, forming the $Cu(II)_B$-OOH intermediate and regenerating a molecule of O_2. This alternative would require superoxide to channel over a much shorter distance via the Y79-assisted pathway and provides a mechanistic role for dioxygen bound at Cu_B, thereby rationalizing our finding that CO binds strongly to the Cu_B center.

The mechanism by which substrate binding induces the proposed switch in O_2 reactivity at Cu_A remains obscure. A substrate-mediated change in the charge within the active-site pocket might induce changes in reactivity of the Cu_A center. This latter speculation is attractive since binding of substrate will neutralize the positive charge on R240, which is equidistant (7 Å) from each copper. Alternatively, it is noteworthy that the evidence for substrate binding near Cu_B comes from crystallographic studies on the oxidized protein, and it is possible that in the reduced form substrate might bind in a different location, closer to Cu_A. In support of this idea, we note that the infrared frequency of the CO ligand

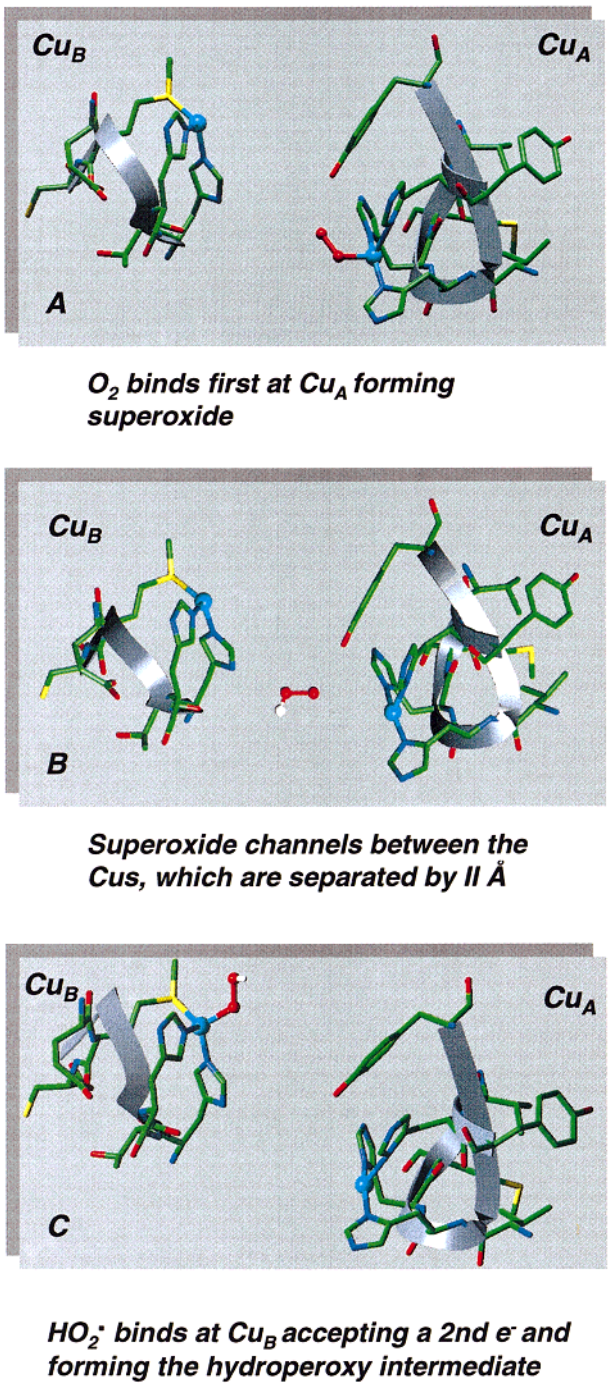

FIGURE 6: A proposed mechanism for superoxide channeling between the two copper centers of PHMcc.

bound at Cu_B (2093 cm^{-1}) is unaffected by substrate binding, whereas ν(CO) for the substrate-induced Cu_A−CO complex is extremely sensitive to the nature of the substrate (hippuric acid, 2075 cm^{-1}; N-AcYVG, 2062, cm^{-1}). This suggests that in the reduced enzyme the substrate does not bind at the crystallographically defined position close to Cu_B, since the ~4 Å approach of the pro-S hydrogen atom to the CO ligand would be expected to perturb the frequency. Rather, a structural and/or electronic interaction of the substrate with the Cu_A-carbonyl seems necessary to produce the observed sensitivity of ν(CO) to substrate structure. Further studies are underway to clarify these and other intriguing features of the PHM mechanism.

ACKNOWLEDGMENT

We thank Drs. Richard E. Mains and Betty E. Eipper for kindly providing us with cell lines, as well as for many stimulating discussions on the expression, structure, and function of PHMcc. We also thank Drs. Sean Prigge and Mario Amzel for making available a restricted set of coordinates for PHMcc prior to deposition in the PDB. We gratefully acknowledge the use of facilities at the Stanford Synchrotron Radiation Laboratory (SSRL), which is supported by the National Institutes of Health Biomedical Research Technology Program, Division of Research Resources, and by the Department of Energy [Basic Energy Sciences (BES) and Office of Biological and Environmental Research (OBER)].

NOTE ADDED IN PROOF

Amzel and coworkers have recently published an X-ray crystal structure of the reduced enzyme. From comparisons with the structure of the substrate-bound oxidized form, they have proposed a novel mechanism in which electron transfer between the two coppers is mediated by the bound substrate. [Prigge, S. T., Kolhekar, A. P., Eipper, B. A., Mains, R. E., and Amzel, L. M. (1999) *Nat. Struct. Biol. 6*, 976−983].

REFERENCES

1. Vale, W., Spiess, J., Rivier, C., and Rivier, J. (1981) *Science 213*, 1394−1397.
2. Eipper, B. A., Mains, R. E., and Glembotski, C. C. (1983) *Proc. Natl. Acad. Sci. U.S.A. 80*, 5144−5148.
3. Eipper, B. A., Stoffers, D. A., and Mains, R. E. (1992) *Annu. Rev. Neurosci. 15*, 57−85.
4. Miller, D. A., Sayad, K. U., Kulathila, R., Beaudry, G. A., Merkler, D. J., and Bertelsen, A. H. (1992) *Arch. Biochem. Biophys. 298*, 380−388.
5. Husten, E. J., and Eipper, B. A. (1991) *J. Biol. Chem. 266*, 17004−17010.
6. Husten, E. J., Tausk, F. A., Keutmann, H. T., and Eipper, B. A. (1993) *J. Biol. Chem. 268*, 9709−9717.
7. Katopodis, A. G., Ping, D., and May, S. W. (1990) *Biochemistry 29*, 6115−6120.
8. Bell, J., Ash, D. E., Snyder, L. M., Kulathila, R., Blackburn, N. J., and Merkler, D. J. (1997) *Biochemistry 36*, 16239−16246.
9. Stoffers, D. A., Ouafik, L. H., and Eipper, B. A. (1991) *J. Biol. Chem. 266*, 1701−1707.
10. Southan, C., and Kruse, L. I. (1989) *FEBS. Lett. 255*, 116−120.
11. Francisco, W. A., Merkler, D. J., Blackburn, N. J., and Klinman, J. P. (1998) *Biochemistry 37*, 8244−8252.
12. Klinman, J. P. (1996) *Chem. Rev. 1996*, 2541−2561.
13. Freeman, J. C., Villafranca, J. J., and Merkler, D. J. (1993) *J. Am. Chem. Soc. 115*, 4923−4924.
14. Kulathila, R., Consalvo, A. P., Fitzpatrick, P. F., Freeman, J. C., Snyder, L. M., Villafranca, J. J., and Merkler, D. J. (1994) *Arch. Biochem. Biophys. 311*, 191−195.
15. Boswell, J. S., Reedy, B. J., Kulathila, R., Merkler, D. J., and Blackburn, N. J. (1996) *Biochemistry 35*, 12241−12250.
16. Eipper, B. A., Quon, A. S. W., Mains, R. E., Boswell, J. S., and Blackburn, N. J. (1995) *Biochemistry 34*, 2857−2865.
17. Yonekura, H., Anzai, T., Kato, I., Furuya, Y., Shizuta, S., Takasawa, S., and Okamoto, H. (1996) *Biochem. Biophys. Res. Commun. 218*, 495−499.
18. Kolhekar, A. S., Keutman, H. T., Mains, R. E., Quon, A. S. W., and Eipper, B. A. (1997) *Biochemistry 36*, 10901−10909.
19. Prigge, S. T., Kolhekar, A. S., Eipper, B. A., Mains, R. E., and Amzel, L. M. (1997) *Science 278*, 1300−1305.
20. Reedy, B. J., and Blackburn, N. J. (1994) *J. Am. Chem. Soc. 116*, 1924−1931.
21. Gray, H. B., and Winkler, J. R. (1996) *Annu. Rev. Biochem. 65*, 537−561.
22. Blackburn, N. J., Pettingill, T. M., Seagraves, K. S., and Shigeta, R. T. (1990) *J. Biol. Chem. 265*, 15383−15386.
23. Pettingill, T. M., Strange, R. W., and Blackburn, N. J. (1991) *J. Biol. Chem. 266*, 16996−17003.
24. George, G. N. (1990) http://ssrl.slac.stanford.edu/exafspak.html.
25. Binsted, N., Gurman, S. J., and Campbell, J. W. (1988) *Daresbury Laboratory EXCURV88 Program*.
26. Gurman, S. J. (1989) in *Synchrotron Radiation and Biophysics* (Hasnain, S. S., Ed.) pp 9−42, Ellis Horwood Ltd., Chichester, U.K.
27. Gurman, S. J., Binsted, N., and Ross, I. (1984) *J. Phys. C: Solid State Phys. 17*, 143−151.
28. Gurman, S. J., Binsted, N., and Ross, I. (1986) *J. Phys. C*: *Solid State Phys. 19*, 1845−1861.
29. Blackburn, N. J., Hasnain, S. S., Pettingill, T. M., and Strange, R. W. (1991) *J. Biol. Chem. 266*, 23120−23127.
30. Sanyal, I., Karlin, K. D., Strange, R. W., and Blackburn, N. J. (1993) *J. Am. Chem. Soc. 115*, 11259−11270.
31. Strange, R. W., Blackburn, N. J., Knowles, P. F., and Hasnain, S. S. (1987) *J. Am. Chem. Soc. 109*, 7157−7162.
32. Fajer, L. Y., and Alben, J. O. (1972) *Biochemistry 11*, 4786−4792.
33. Alben, J. O., Moh, P. P., Fiamingo, F. G., and Altschuld, R. A. (1981) *Proc. Natl. Acad. Sci. U.S.A. 78*, 234−237.
34. Dyer, R. B., Einarsdottir, O., Killough, P. M., Lopez, G. J. J., and Woodruff, W. H. (1989) *J. Am. Chem. Soc 111*, 7657−7659.
35. Hosler, J. P., Kim, Y., Shapleigh, J., Gennis, R., Alben, J., Ferguson, M. S., and Babcock, G. (1994) *J. Am. Chem. Soc 116*, 5515−5516.
36. Puustinen, A., Bailey, J. A., R. B., D., Mecklenburg, S. L., Wikstrom, M., and Woodruff, W. H. (1997) *Biochemistry 36*, 13195−13200.
37. Pasquali, M., and Floriani, C. (1984) in *Copper Coordination Chemistry, Biochemical and Inorganic Perspectives* (Karlin, K. D., and Zubieta, J., Eds.) pp 311−330, Adenine Press, New York.
38. Patch, M. G., Choi, H., Chapman, D. R., Bau, R., McKee, V., and Reed, C. A. (1990) *Inorg. Chem. 29*, 110−119.
39. Villacorta, G. M., and Lippard, S. J. (1987) *Inorg. Chem. 26*, 3672−3676.
40. Sorrell, T. N., and Malachowski, M. R. (1983) *Inorg. Chem. 22*, 1883−1887.
41. Sorrell, T. N., and Borovick, A. S. (1987) *J. Am. Chem. Soc. 109*, 4255−4260.
42. Volbeda, A., and Hol, W. G. J. (1989) *J. Mol. Biol. 209*, 249−279.
43. Cuff, M. E., Miller, K. I., van Holde, K. E., and Hendrickson, W. A. (1998) *J. Mol. Biol. 278*, 855−870.
44. Hazes, B., Magnus, K., A., Bonaventura, C., Bonaventura, J., Dauter, Z., Kalk, K. H., and J., H. W. G. (1993) *Protein Sci. 2*, 597−619.
45. Klabunde, T., Eicken, C., Sacchettini, J. C., and Krebs, B. (1998) *Nature Struct. Biol. 5*, 1084−1090.
46. Xie, B., Elder, T., Wilson, L. J., and Stanbury, D. M. (1999) *Inorg. Chem. 38*, 12−19.
47. Winkler, J. R., and Gray, H. B. (1992) *Chem. Rev. 92*, 369−379.
48. Holm, R. H., Kennepohl, P., and Solomon, E. I. (1996) *Chem. Rev. 96*, 2239−2314.
49. Dunn, B. C., Ochrymowycz, L. A., and Rorabacher, D. B. (1995) *Inorg. Chem. 34*, 1954−1956.
50. Dunn, B. C., Wijetunge, P., Vyvyan, J. R., Howard, T. A., Grall, A. J., Ochrymowycz, L. A., and Rorabacher, D. B. (1997) *Inorg. Chem. 36*, 4484−4489.
51. Dunn, B. C., Ochrymowycz, L. A., and Rorabacher, D. B. (1997) *Inorg. Chem. 36*, 3253−3257.
52. Sisley, M. J., and Jordan, R. B. (1992) *Inorg. Chem. 31*, 2880−2884.

BI991341W